Probing exotic spin correlations by muon spin depolarization measurements with applications to spin glass dynamics

Amit Keren,[1] Galina Bazalitsky,[1] Ian Campbell,[2] and James S. Lord[3]
[1]*Physics Department, Technion–Israel Institute of Technology, Haifa 32000, Israel*
[2]*Laboratoire des Verres, Université Montpellier II, 91405 Montpellier, France*
[3]*Rutherford Appleton Laboratory, Chilton Didcot, Oxfordshire OX11 0QX, United Kingdom*
(Received 15 February 2001; published 29 June 2001)

We develop a method to probe the local spin dynamic autocorrelation function, using magnetic-field-dependent muon depolarization measurements. We apply this method to muon spin relaxation experiments in the dilute Heisenberg spin glass AgMn (p at. %) at $T>T_g$, where the correlations of the Mn local magnetic moment are strongly nonexponential. Our results clearly indicate that the dynamics of this spin glass cannot be described by a distribution of correlation times. Therefore, we analyze the data assuming a local spin correlation function which is the product of a power law times a cutoff function. The concentration and temperature dependence of the parameters of this function are determined. Our major conclusion is that in the temperature region close to T_g the correlation function is dominated by an algebraic relaxation term.

DOI: 10.1103/PhysRevB.64.054403 PACS number(s): 75.10.Nr, 76.20.+q, 76.75.+i

I. INTRODUCTION

In the vicinity of a second order magnetic phase transition, the spin-spin dynamical autocorrelation function

$$\langle \mathbf{S}_i(t)\mathbf{S}_i(0)\rangle \equiv q(t), \tag{1}$$

must take the general form[1]

$$q(t)\sim t^{-x}f(t/\tau). \tag{2}$$

In these equations i is a site index, $\langle\ \rangle$ is a thermal and sample average, τ is a time scale that limits the upper range of the decay, x can be defined in terms of the static and dynamic critical exponents, and f is a ''cutoff'' function, which can take different forms. In simple systems, such as isolated spins, the power law part does not exist ($x=0$), and f is exponential, making $q(t)$ exponential. In systems with interacting spins $q(t)$ can be nonexponential. For example, in a pure ferromagnet close to T_c, $q(t)$ is given by Eq. (2) with $x>0$ and exponential f. In this case, the correlation function of all individual spins is the same as the global one by definition. In complex systems, with physical properties such as time scale invariance[2] or hierarchical relaxation,[3] $q(t)$ can be *strongly* nonexponential. An important example is spin glasses with frozen-in disorder, where the local environments of individual spins are not identical. In this case numerical simulations show that the global correlation function also takes the form of Eq. (2) but f is a stretched exponential.[4,5] In addition, these simulations show that Eq. (2) is valid even locally but f varies from spin to spin. Therefore, they have been analyzed with more complex cutoff functions, such as a sum of exponentials[6] or a sum of stretched exponentials.[7]

Despite this theoretical understanding of the correlation function, the complex nature of $q(t)$ is frequently ignored in the analysis of experimental systems and they are interpreted in terms of a sum of exponential relaxation rates: some spins are relaxing fast and some slowly. Indeed, the Laplace transform of any relaxation function $q(t)$ can always be defined in terms of a spectrum of relaxation times. However, the relaxation times of the distribution are those of the modes of the system, not those of the individual spins. (To take a familiar analogy, in a pure crystal there is a spectrum of phonon modes but any atom is vibrating in precisely the same complex way as any other atom.)

In this work we avoid the assumption of a distribution of correlation times and determine $q(t)$ experimentally using the alternative hypothesis of a unique nonexponential $q(t)$. For reasons described in Sec. II our technique of choice is muon spin relaxation (μSR). Muons are implanted in a sample initially fully polarized and are depolarized in the neighborhood of local magnetic moments. The form of the muon depolarization is a signature of $q(t)$. The practical difficulty is to establish in the general case an inversion scheme that can take one unambiguously from the muon depolarization pattern back to the correlation function. Accordingly, our main objectives in this work are (I) to develop (in Sec. III) a method by which one can determine the functional form of $q(t)$ by measuring both the field and time dependence of the muon polarization $P(H,t)$; (II) to apply this method to a real Heisenberg spin glass and to determine x and τ (see Sec. IV).

This work is a continuation of our previous publication where we demonstrated the existence of an unusual correlation function in the spin glass AgMn (0.5 at. %) at $T>T_g$ at a single temperature.[8] There it was shown that at high fields (>120 G) and late times, the muon polarization obeys the scaling relation

$$P(H,t)=P(t/H^{1-x}), \tag{3}$$

and this relation was traced back to the correlation function given by Eq. (2). However, an interpretation of the parameters x and τ was not provided, and no attempt was made to discuss the singularity of $q(t)$ at $t=0$. Here we extend Ref. 8 in four different directions: (I) we address the $t=0$ singularity, (II) we apply lower fields where $P(H,t)$ is most sensitive to f, (III) we vary the temperatures, and (IV) we ex-

amine three different samples of AgMn (p at. %) with $p=0.1$, 0.3, and 0.5 where $T_g=0.51$, 1.45, and 2.80 K, respectively. This allows us to estimate the various parameters of $q(t)$ as a function of p and T. Our most important finding is that $q(t)$ depends on temperature mainly through $x(T)$ in these samples.

II. EXPERIMENTAL ASPECTS AND RAW DATA

As demonstrated in Ref. 8 and derived again in Sec. III a clear evidence for an exotic correlation function is the scaling relation of Eq. (3). In order to find this type of scaling experimentally from the raw muon spectra with good certainty, one must vary the external field over two orders of magnitude. The μSR technique is especially well adapted for this task since the signal intensity is independent of H, and one can vary the magnetic field considerably, the upper limit being given by the fields available in the experimental setups, and the lower limit being related to the range of applicability of the analysis method. In addition, experiment shows that the typical time scales are of the order of a microsecond, which falls between the ranges covered conveniently by neutron techniques and by conventional susceptibility techniques.

Our μSR experiments were performed in ISIS where magnetic fields up to 4 kG are available. In these experiments we measure the time- and field-dependent asymmetry $A(H,t)$ of the decay positrons in the directions parallel and antiparallel to the initial muon polarization. This asymmetry is proportional to $P(H,t)$ where H is applied in the direction of the initial polarization, and $P(H,0)=1$; for more details see Ref. 8. The fields applied for each sample obey the condition $\mu_{eff}H<T_g$, where μ_{eff} is the magnetic moment of the Mn ions. This condition ensures that the impact of the fields on the local moment correlation function is minimal. Standard frequency-dependent susceptibility measurements on spin glasses show that a magnetic field has negligible effect on the spin glass relaxation, even at quite low frequencies corresponding to times of the order of a millisecond; as the μSR technique is intrinsically limited to time scales of the order of a microsecond or less, we can safely ignore any direct effects of magnetic fields on the local moment relaxation.

We have used AgMn since Ag nuclear moments are negligible and there is no need to worry about background relaxation from Ag nuclei. Although dilute, the Mn nuclear moments are large and it turns out that the Mn nuclear term can influence the muon depolarization signal in zero applied field. The samples were prepared by melting in a sealed quartz tube, followed by strong cold work. The samples were transformed from buttons to sheets about 0.2 mm thick and were then annealed for a week under vacuum. This technique is standard for ensuring complete homogenization. The glass transition temperatures were determined using a standard ac-susceptibility method. For the $p=0.3$ and $p=0.1$ concentrations we were assisted by the dilution refrigerator of C. Paulsen in Grenoble.

Representative $A(H,t)$ measurements in the $p=0.5$ and 0.1 samples at $T=2.9$ and 0.6 K, respectively, and at various fields, are shown in Fig. 1 panels (a) and (b). Clearly, H affects the muon polarization very strongly over more than two orders of magnitude. The larger H the weaker the relaxation. This well known effect is called decoupling. The scaling relations of Eq. (3) are shown to hold with $x\to 0$ at high fields and late times for the $p=0.5$ sample in Fig. 2. Our aim is to account for the rate of decoupling, namely, the scaling relations, quantitatively.

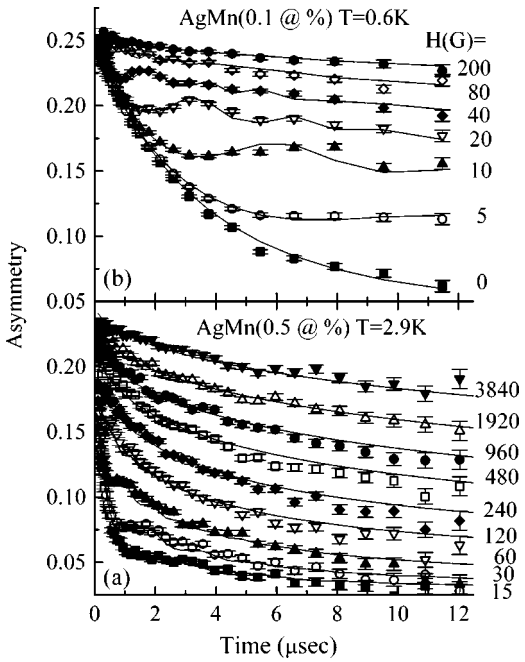

FIG. 1. Asymmetry vs time in two samples for various longitudinal magnetic fields. The solid lines are fits to the model described in the text.

III. ANALYSIS

First we would like to emphasize the need for a different type of analysis for our data. In the Appendix we show that the muon polarization is determined by the field-field dynamical autocorrelation function

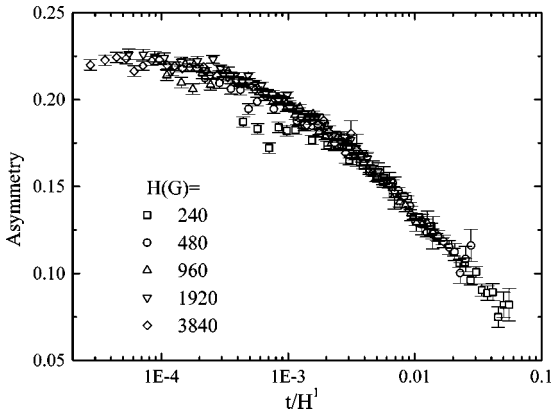

FIG. 2. The asymmetry from Fig. 1(a) plotted as a function of t/H^1 for fields higher than 240 G. This plot demonstrates the experimental validity of Eq. (3) with $x\to 0$.

$$\Phi(t) \equiv \gamma_\mu^2 \langle \mathbf{B}_\perp^d(t) \cdot \mathbf{B}_\perp^d(0) \rangle$$

(rather than by q), where $\mathbf{B}_\perp^d$ is the dynamic magnetic field at the muon site perpendicular to the external field $\mathbf{H}$, and $\gamma_\mu = 85.16$ MHz/kG is the muon gyromagnetic ratio. In the high field and late time limit we arrive at the relation

$$P(H,t) = P[t/T_1(H)], \tag{4}$$

where

$$\frac{1}{T_1(H)} = \int_0^\infty \Phi(t') \cos(\gamma H t') dt'. \tag{5}$$

Since in a spin glass there are no cross correlations between spins one expects $\Phi(t) \propto q(t)$. Therefore, for an exponential correlation function $q(t)$ with a single correlation time we write

$$\Phi(t) = 2\Delta^2 \exp(-t/\tau), \tag{6}$$

where

$$2\Delta^2 = \gamma_\mu^2 \langle \mathbf{B}_\perp^2 \rangle.$$

In this case the muon relaxation rate is given by the known expression

$$\frac{1}{T_1(H)} = \frac{2\Delta^2 \tau}{1 + (\gamma_\mu \tau H)^2}.$$

However, in a spin glass, the muon could stop in a variety of environments and can experience different instantaneous fields or correlation times. If we allow for a distribution of Δ and/or τ we can obtain an average polarization $\overline{P}$ by

$$\overline{P}(H,t) = \int \int \rho(\Delta,\tau) P\left(\frac{2\Delta^2 \tau t}{1 + (\gamma_\mu \tau H)^2} \right) d\Delta\, d\tau.$$

Nevertheless, if $\gamma_\mu H \gg 1/\tau^{\min}$, where $\tau^{\min}$ is the shortest correlation time in the distribution, we expect

$$P(H,t) = P(t/H^2),$$

which is in contrast to the experimental observation depicted in Fig. 2. This brings us to one of the important conclusions of our experiments: a distribution of correlation times could not explain our data.

The second problem with the standard analysis method emerges from the ''wiggles'' seen in the data at early times and low fields. These could not be accounted for by Eq. (4), which does not have oscillating terms. The source of the oscillations are those muons for which the transverse magnetic field has not relaxed abruptly during the time of one rotation. These muons will oscillate around the vector sum of both internal and external fields at a frequency $\omega = \gamma_\mu \sqrt{H^2 + B_\perp^d}$. Since at $T > T_g$ there is a distribution of B^d with zero average, the contribution of the dynamic field will show up as a relaxation of the wiggles, while the frequency of the wiggles will be at $\omega = \gamma_\mu H$. Roughly, if there is a cutoff time τ, then by the time $t > \tau$ abrupt field relaxation occurs for all muons. Therefore, the wiggle pattern will not be seen for longer times. As a result, the observation of a wiggle pattern up to time t is a proof of local moments that do not relax abruptly within this time scale, and so gives a model-independent estimate of τ. The fit procedure described below provides a quantitative method to include this type of observation within the global analysis of the field-dependent muon depolarization.

Having demonstrated that neither the field-time scaling relations nor the wiggles in the data could be accounted for with standard analysis methods we turn to describing our alternative approach. If one does not take the long time limit that led to Eqs. (4) and (5), one finds (see the Appendix) that the relation between $P(H,t)$ and $\Phi(t)$ is via the expression

$$P(H,t) = P_0 \exp[-\Gamma(H,t)t], \tag{7}$$

where

$$\Gamma(H,t)t = \int_0^t (t-t') \Phi(t') \cos(\gamma_\mu H t') dt'. \tag{8}$$

This expression can produce the oscillations seen in the data [for the exponential case given by Eq. (6) see Ref. 9]. Motivated by the success of Eq. (2) in accounting for the preliminary data of Ref. 8 we examine here the correlation function

$$\Phi(t) = 2\Delta^2 \frac{\tau_e^x}{(t+\tau_e)^x} \exp(-t/\tau_l), \tag{9}$$

where τ_e and τ_l are an early and late time cutoff, respectively. This $\Phi(t)$ is properly normalized at $t=0$. From neutron spin echo data,[10] τ_e is of the order of 1 ps, and approximately independent of temperature. Therefore, we are safe to assume that the time at which the muon polarization is first measured (0.1 μs) is much longer than τ_e. In other words, our experiment is in the limit of $t \gg \tau_e$, and we can write

$$\Phi(t) = 2C\iota(t),$$

where

$$C = \Delta^2 \tau_e^x$$

and

$$\iota(t) = t^{-x} \exp(-t/\tau_l). \tag{10}$$

Now we express

$$\Gamma(H,t)t = 2\Delta^2 \tau_e^x \int_0^t (t-t')\, \iota(t') \cos(\gamma H t') dt'. \tag{11}$$

To be rigorous we should allow for a distribution of all the parameters in the correlation function. This, of course, will lead us nowhere. Therefore, we assume only a distribution of Δ and so assume a unique form of $q(t)$ for all local spins. This assumption appears physically reasonable and as we shall see it allows us to account for our data successfully. We note that all μSR data to date were analyzed using this assumption, and, in particular, the following distribution[11] was chosen:

$$\rho(\Delta)=\sqrt{\frac{1}{2\pi}}\frac{\Delta^*}{\Delta^2}\exp\left(-\frac{1}{8}\left[\frac{\Delta^*}{\Delta}\right]^2\right). \tag{12}$$

As before the average muon polarization $\overline{P}$ is given by

$$\overline{P}(H,t)=P_0\int \rho(\Delta)\exp[-\Gamma(H,t)t]d\Delta,$$

which leads to

$$\overline{P}(H,t)=P_0\ \exp(-[\Gamma^*(H,t)t]^{1/2}), \tag{13}$$

where

$$\Gamma^*(H,t)t=2C^*\int_0^t(t-t')\iota(t')\cos(\gamma Ht')dt', \tag{14}$$

and

$$C^*=(\Delta^*)^2\tau_e^x. \tag{15}$$

The difference between P before averaging over Δ and $\overline{P}$ (after the average) is fundamental and is manifested in the appearance of a power 1/2 in the exponent of Eq. (13). In fact, the reason for choosing $\rho(\Delta)$ given by Eq. (12) is that experimental data agree well with Eq. (13). In contrast, the difference between Γ and Γ^* is minor; C is simply replaced by C^*, namely, Δ is replaced by Δ^*. In reality we do not use Eq. (13) but rather fit our data to

$$\overline{P}(H,t)=P_0\ \exp(-[\Gamma^*(H,t)t]^{\beta}) \tag{16}$$

with $\beta\sim 1/2$ a global parameter for all samples and temperatures.

It is instructive to examine Eqs. (16) and (14) numerically for a particular example of $\iota(t)$. The integral of Eq. (14) is well defined and could be evaluated by the improper integration method.[12] In Fig. 3(a) we depict the numerical $P(\omega,t)$ vs t for various values of $\omega=\gamma_p H$ where the parameters of the correlation function are $C^*=1$, $x=0.3$, $\tau_l=3.3$, and in Eq. (16) $\beta=0.5$ (for other cases, see Ref. 13). There are two important features in this figure. First, at low frequencies there are pronounced wiggles in the simulation waveform at early times, as in the data. The time scale on which wiggles are observed (t_w), which is demonstrated on the graph, obeys $t_w\lesssim\tau_l$. Therefore, as mentioned before, τ_l could be estimated by visually inspecting the low field, early time data. Second, there is absolutely no difference in the polarization between $\omega=0$ and $\omega=0.3$. In other words, at low fields the polarization is field independent and the field impacts the polarization only for $\omega>1/\tau_l$. This provides a complementary qualitative method of estimating τ_l. In fact, both methods are well known for the pure exponential correlation function. The point being made here is that these methods are correct even when a power law multiplies the exponential decay term in the expression for $q(t)$, so direct observation of the threshold value of the field dependence of the polarization is a complementary, model-independent method of estimating the cutoff time.

In Fig. 3(b) we show the numerical $P(\omega,t)$ vs $t/\omega^{0.7}$ for $\omega\geqslant 5$. Clearly, at high enough frequencies and late enough

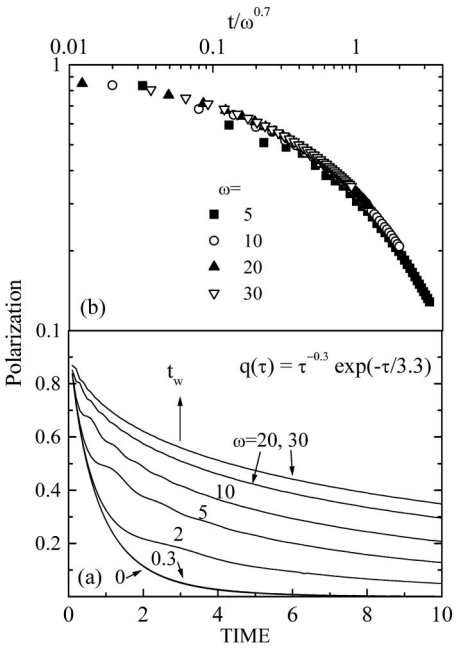

FIG. 3. (a) The polarization generated using Eqs. (10), (13), and (14), for various frequencies $\omega=\gamma_\mu H$. (b) Demonstrating the theoretical validity of Eq. (3) for high enough values of $\omega=\gamma_\mu H$ and late times.

times scaling of the form of Eq. (3) indeed holds. The critical value above which H and t are considered large is determined by τ_l. Late time is $t>\tau_l$, and high fields are $H>(\gamma_\mu\tau_l)^{-1}$. It is therefore very important to observe wiggles and/or a strong field effect in the data (e.g., Fig. 1) before the cutoff time and x can be obtained unambiguously from the scaling.

We now apply these concepts to the analysis of our μSR data. The analysis of the measurements shown in Fig. 1(a) is discussed in detail using four steps. First, we estimate τ_l. The wiggles in the waveform prevail for $t_w\sim 2$ μs, and fields as small as 30 G ($\omega=2.5$ MHz) impact the polarization. Both these observations indicate that τ_l is of the order of 1 μs. Second, we evaluate x. From the value of τ_l we expect scaling to hold for $t>1$ μs and for fields bigger than 100 G. Indeed, in Fig. 2 when $t/H^1>0.01$ (and even much earlier) all data sets collapse onto one line, meaning $x\to 0$ (as mentioned before). Third, we estimate C^* and β. By expanding $\iota(t)$ in powers of t, performing the integral of Eq. (14) term by term for the zero field case ($H=0$), and keeping only the first term we find that

$$\Gamma^*(0,t)t=\frac{2C^*t^{2-x}}{(2-x)(1-x)}+O(t^{3-x}).$$

Using this relation in Eq. (16), and fitting the lowest field, early time data to a stretched exponential (while holding x fixed from the second step), we can obtain C^* and β. The values found up to now for C^*, x, τ_l, and β are used as initial guesses for a global fit (at a given T) for all applied fields. In the global fit we allow freedom in H for fields $\leqslant 30$ G in order to account for the sample's susceptibility and demagnetization, and also since our power supply does not

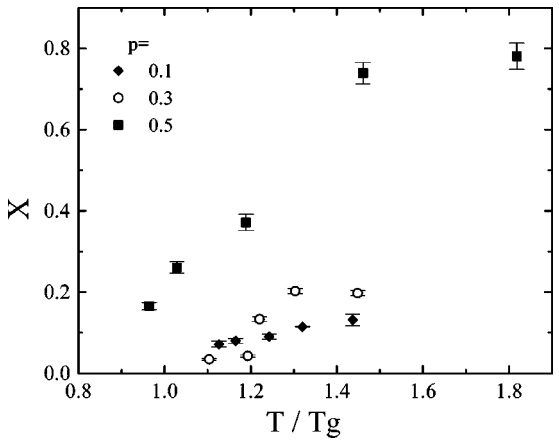

FIG. 4. x [from Eq. (10)] plotted vs temperature for different samples.

give accurate values in such small fields. The global fit produces values of x somewhat larger than those obtained from scaling and smaller error bars. The results of this fit procedure are presented in Fig. 1(a) by the solid lines. Our model captures the essence of the wiggles, although for some fields it fails to capture the fine details of the waveform at early times. More importantly, the model accounts very well for the data past the wiggles for more than 2.5 orders of magnitude in field. The same analysis method is applied to our series of samples at various temperatures. We find that $\beta = 0.45(5)$ globally for all samples and temperatures. A second example of the success of this analysis procedure is depicted in Fig. 1(b) by the solid lines.

At first sight it would appear that with so many fit parameters no significant conclusions could be reached. In fact, because a single set of fit parameters is being used to fit a whole family of curves and because different parameters dominate the behavior at different ranges of time and field, the fit parameters are well pinned down. There is some interplay between different parameters so the values are correlated, but it turns out that the conclusions that we will reach (relaxation dominated by x, cutoff times comparable to or longer than a microsecond) are robust. To get fully reliable and unique fits, certain purely experimental parameters (background and initial anisotropy for the whole range of fields used) must be well established from independent control runs.

IV. RESULTS

We now turn to discuss the outcome of the fits. The power x is plotted vs T/T_g in Fig. 4. At all temperatures studied (from T_g to about $2T_g$) we find x values that are clearly bigger than zero, and increase with increasing T, in qualitative agreement with Ogielski's simulations[4] and with the more recent results of Franzese and Coniglio.[5] In general, at a given T/T_g, the power x appears to increase with increasing magnetic ion concentration p. Theoretically, near a continuous phase transition the power x is expected to relate to the static and dynamic critical exponents through $x=(d+\eta)/2z$[4]. We find x values that are of the order of 0.15 close

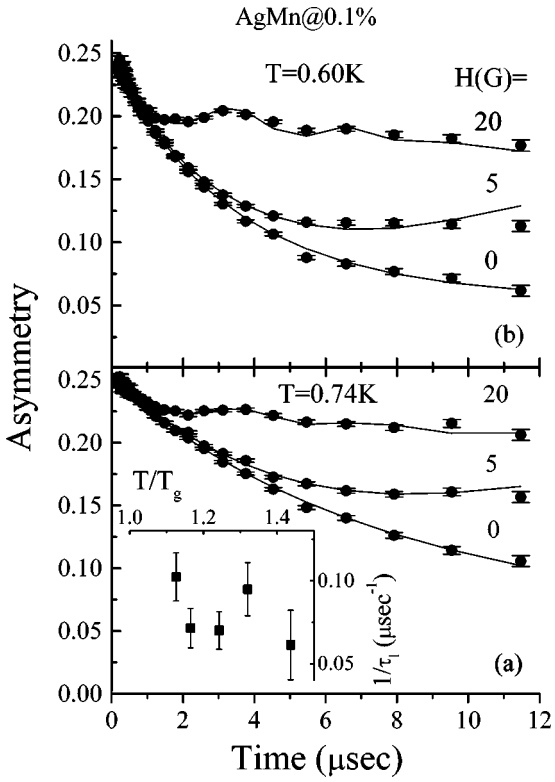

FIG. 5. Demonstrating that neither the wiggling time t_w nor the sensitivity of the polarization to the field are varying with temperature. The inset shows the late cutoff time τ_l as given by Eq. (10) versus T/T_g for the $p=0.1$ sample.

to T_g. This should be compared with the value of 0.13 that can be estimated from exponents obtained by magnetic measurements at low frequencies on the same type of alloy.[14] This exponent could be expected to be independent of concentration for dilute alloys.

As for the cutoff time τ_l, we have noticed that τ_l changes little as a function of the temperature over the temperature range we have studied. This is best demonstrated in the $p=0.1$ sample where the waveform has strongest wiggles and strong field dependence, and is therefore most sensitive to τ_l. In Figs. 5(a) and 5(b) we present $P(H,t)$ at three representative fields and two different temperatures approaching T_g. Clearly, a field as small as 5 G ($\omega=0.4$ MHz) impacts the polarization at both temperatures, and there is no big change in the wiggle time t_w ($\sim 10\ \mu$s) between these temperatures. Thus τ_l remains longer than a few microseconds up to $T/T_g=1.43$. In the inset of Fig. 5(a) we show the fit results for $1/\tau_l$ for the $p=0.1$ sample, demonstrating once again that we do not observe a critical temperature dependence. On general physical principles related to any continuous transition, τ_l should diverge as T tends to the ordering temperature (see, for instance, Ogielski's Ising spin glass simulations[4]). The present data simply indicate that for the concentrations and temperature ranges studied τ_l is at the edge or out of the muon dynamic window.

Finally, we examine the parameter C^*. The mean square of the field $\langle \mathbf{B}_\perp^2 \rangle$ (or Δ^2) at a given site should be T independent, and so should $(\Delta^*)^2$. If τ_e is also T independent,

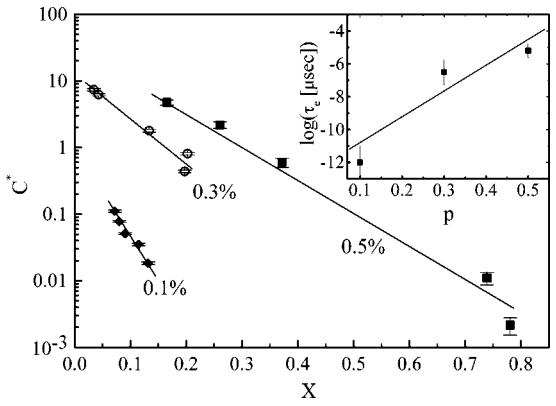

FIG. 6. The prefactor C^* plotted versus x on a semilogarithmic scale [see Eq. (15)]. The temperature is an implicit parameter. The solid curves are linear fits. Their slope is interpreted as $\log_{10}\tau_e$ and presented in the inset.

we expect from Eq. (15) a $\log_{10}(C^*)$ against x plot to be a straight line. Indeed, a linear dependency between $\log_{10}(C^*)$ and x is consistent with the data as shown in Fig. 6. The slope of the line at each concentration is $\log_{10}\tau_e$ and the intercept is $2\log_{10}(\Delta^*)$. The values of the intercepts have large error bars (since we do not have data at sufficiently small x) and are therefore not presented. Nevertheless, a rough estimate of Δ^* indicates that the condition for validity of our analysis, namely, $H>\Delta^*$ (see the Appendix) holds for $H\gtrsim 10$ G for the $p=0.5$ and 0.3 samples, and $H\gtrsim 1$ G for the $p>0.1$ sample as done here. The values of $\log_{10}\tau_e$ are presented in the inset of Fig. 6 for the different samples. These values make the conjecture $t\gg\tau_e$ self-consistent, although we find τ_e for the $p=0.1$ sample unacceptably small. Nevertheless, our analysis indicates that the T dependence of C^* is due only to $x(T)$.

To summarize, we demonstrate that a distribution of correlation times cannot account for the muon polarization as a function of both field and time. However, we can account for our data provided that each muon experience a local field correlation function given by Eq. (9), where the only difference between different muons is in the value of Δ. Our analysis shows that out of all the parameters that determine $P(H,t)$, namely, x, τ_l, τ_e, and Δ^*, the only one that is temperature dependent is x. We thus conclude that the dynamic behavior of this family of dilute spin glasses near T_g is controlled essentially by the temperature dependence of the power law exponent x.

ACKNOWLEDGMENTS

We would like to thank the ISIS facility for its hospitality. This research was supported by the Israeli Academy of Science, and by the EU TMR program. We also would like to thank C. Paulsen for measuring T_g in our low concentration samples using his dilution refrigerator.

APPENDIX FROM FIELD CORRELATIONS TO SPIN LATTICE RELAXATION

In this Appendix we derive the expected behavior of the polarization of a local probe, which is out of equilibrium, in a dynamic field environment. For simplicity we use a semiclassical approach. A more complete result, based on a full quantum treatment, can be found in the literature[15] but there is no detectable difference. In the semiclassical method we decompose the Hamiltonian of a spin 1/2 experiencing both an external static field H and an internal dynamically fluctuating field $\mathbf{B}^d(t)$ into

$$\mathcal{H}=\mathcal{H}_0+\mathcal{H}'(t), \tag{A1}$$

where

$$\mathcal{H}_0=-\gamma_\mu S_z H \tag{A2}$$

is the secular part, and the interaction part is

$$\mathcal{H}'=-\gamma_\mu \mathbf{S}\cdot\mathbf{B}^d(t). \tag{A3}$$

The time-dependent field $\mathbf{B}^d(t)$ is taken to be classical and $\mathbf{S}$ is the muon spin operator. When the fluctuating fields are smaller than the external field we can use time-dependent perturbation theory and write the time propagator as

$$U(t)=\exp\left(-\frac{i}{\hbar}\mathcal{H}_0 t\right)\left[1-\frac{i}{h}\int_0^t dt'\,\mathcal{H}^{\mathrm{I}}(t') -\frac{1}{h^2}\int_0^t dt'\int_0^{t'} dt''\mathcal{H}^{\mathrm{I}}(t')\mathcal{H}^{\mathrm{I}}(t'')+\cdots\right], \tag{A4}$$

where the perturbation Hamiltonian in the interaction picture is given by

$$\mathcal{H}^{\mathrm{I}}(t)=\exp(i\mathcal{H}_0 t/\hbar)\mathcal{H}'(t)\exp(-i\mathcal{H}_0 t/\hbar). \tag{A5}$$

This Hamiltonian simplifies to

$$\mathcal{H}^{\mathrm{I}}(t)=-\gamma_\mu \mathbf{B}^d(t)\mathbf{S}^{\mathrm{I}}(t), \tag{A6}$$

where

$$\mathbf{S}^{\mathrm{I}}(t)=\exp(i\omega S_z t/\hbar)\mathbf{S}\,\exp(-i\omega S_z t/\hbar)$$

and

$$\omega=-\gamma_\mu H.$$

Explicitly $\mathbf{S}^{\mathrm{I}}(t)$ is given by

$$\begin{aligned} S_x^{\mathrm{I}}(t)&=S_x\cos(\omega t)-S_y\sin(\omega t),\\ S_y^{\mathrm{I}}(t)&=S_y\cos(\omega t)+S_x\sin(\omega t),\\ S_z^{\mathrm{I}}(t)&=S_z. \end{aligned} \tag{A7}$$

Note that $\mathbf{S}^{\mathrm{I}}(t)$ is the time-dependent spin operator in the interaction picture, namely, of a muon that rotates around the external field as if there were no internal fields. It is not the spin operator $\mathbf{S}(t)$ of a muon that experiences the combined static and dynamic fields. In other words, in order to find $\mathbf{S}(t)$ we use a perturbation expansion in terms of $\mathbf{S}^{\mathrm{I}}(t)$. This is the (mathematical) origin of the wiggles seen in the data at the frequency of the external field.

Using Eqs. (A6) and (A7) we find that

$$\mathcal{H}^{\mathrm{I}}(t)=-\gamma_\mu[V(t)S_x-U(t)S_y+T(t)S_z], \tag{A8}$$

where

$$V(t)=B_x^d(t)\cos(\omega t)+B_y^d(t)\sin(\omega t),$$

$$U(t)=B_x^d(t)\sin(\omega t)-B_y^d(t)\cos(\omega t),$$

$$T(t)=B_z^d(t).$$

The polarization of a muon at a given site as a function of time $P_z(t)$ is given by

$$P_z(t)=\mathrm{Tr}[\rho U^{\dagger}(t)\sigma_z U(t)] \tag{A9}$$

where

$$\rho=\frac{1+P_0\sigma_z}{2}$$

and P_0 is the initial polarization.

Equations (A9) and (A4) lead to the perturbation series

$$P(t)=I+II+III+\cdots, \tag{A10}$$

where

$$I=\mathrm{Tr}\{\rho\sigma_z\},$$

$$II=\frac{i}{\hbar}\int_0^t dt'\,\mathrm{Tr}\,\rho[\mathcal{H}^{\mathrm{I}}(t'),\sigma_z], \tag{A11}$$

$$III=-\frac{1}{\hbar^2}\int_0^t dt'\int_0^{t'} dt''\mathrm{Tr}\,\rho[\mathcal{H}^{\mathrm{I}}(t''),[\mathcal{H}^{\mathrm{I}}(t'),\sigma_z]]..$$

We now evaluate each term explicitly: The first term is simple. Since

$$\mathrm{Tr}\{\rho\sigma_i\}=\begin{cases}P_0, & i=z\\ 0, & i=x,y\end{cases}$$

we get $I=P_0$. In the second term we have

$$[\mathcal{H}^{\mathrm{I}}(t'),\sigma_z]=i\gamma_\mu[V(t')\sigma_y+U(t')\sigma_x].$$

After the evaluation of the trace we find $II=0$. For the third term we find

$$\mathrm{Tr}\,\rho[\mathcal{H}'(t''),[\mathcal{H}'(t'),\sigma_z]]=P_0\gamma_\mu^2[V(t'')V(t')+U(t'')U(t')],$$

where we have used the simplifying assumption that V, U, and T are classical fields. To progress further with the calculation it is helpful to introduce at this stage the ensemble average over all possible trajectories of $\mathbf{B}_\perp^d(t)$. Quantities in $\langle\ \rangle$ will denote such an average and we can write

$$\langle P_z\rangle=\langle I\rangle+\langle III\rangle \tag{A12}$$

where $\langle I\rangle=P_0$ and

$$\langle III\rangle=P_0\gamma_\mu^2\langle V(t'')V(t')+U(t'')U(t')\rangle.$$

The meaning $\langle B_i^d(t')B_j^d(t'')\rangle$ is to hold t' and t'' fixed and to average over all possible fields in the systems between these times. This is a correlation function. We assume that there are no cross correlations and x,y symmetry so the only terms left to evaluate are of the form

$$\langle V(t'')V(t')+U(t'')U(t')\rangle=\langle B_x^d(t')B_x^d(t'')+B_y^d(t')B_y^d(t'')\rangle\cos[\omega(t''-t')].$$

We now make the assumption that the correlation function depends only on the time difference and define

$$\Phi(t'-t'')=\gamma_\mu^2\langle B_x^d(t')B_x^d(t'')+B_y^d(t')B_y^d(t'')\rangle, \tag{A13}$$

so that finally

$$\langle III\rangle=-P_0\int_0^t dt'\int_0^{t'} dt''\Phi(t'-t'')\cos[\omega(t'-t'')]. \tag{A14}$$

We can eliminate one of the integrals by writing

$$\tau=t'-t'',$$

$$\tau'=t-t'.$$

This transforms the integral into

$$\int_0^t dt'\int_0^{t'} dt''=\int_0^t d\tau\int_0^{t-\tau} d\tau'$$

and we arrive at

$$\langle III\rangle=-P_0\int_0^t d\tau(t-\tau)\Phi(\tau)\cos(\omega\tau). \tag{A15}$$

If we now write

$$P_z(t)=P_0\,\exp[-\Gamma(t)t], \tag{A16}$$

expand this equation in powers of Γ, and compare it with Eqs. (A12) and (A15), we find

$$\Gamma(t)t=\int_0^t d\tau(t-\tau)\Phi(\tau)\cos(\omega\tau). \tag{A17}$$

At late times, such that $\Phi(t)$ is negligible, one finds that

$$\Gamma(H,t)\to\frac{1}{T_1(H)}=\int_0^\infty\Phi(\tau)\cos(\omega\tau)d\tau. \tag{A18}$$

[1] P. C. Hohenberg and B. L. Halperin, Rev. Mod. Phys. **49**, 435 (1977).

[2] H. Scher, M. F. Shlesinger, and J. Bendler, Phys. Today **44** (1), 26 (1991); J. Klafter, M. F. Shlesinger, and G. Zumofen, *ibid.* **49** (2), 33 (1996).

[3] R. G. Palmer, D. L. Stein, E. Abrahams, and P. W. Anderson, Phys. Rev. Lett. **53**, 958 (1984).

[4] A. T. Ogielski, Phys. Rev. B **32**, 7384 (1985).

[5] G. Franzese and A. Coniglio, Phys. Rev. E **59**, 6409 (1999).
[6] H. Takayama and H. Yoshino, Physica A **204**, 650 (1994); Hiroshi Takano and Seiji Miyashita, J. Phys. Soc. Jpn. **64**, 560 (1995).
[7] S. C. Glotzer, N. Jan, T. Lookman, A. B. MacIsaac, and P. H. Poole, Phys. Rev. E **57**, 7350 (1998).
[8] A. Keren, P. Mendels, I. A. Campbell, and J. Lord, Phys. Rev. Lett. **77**, 1386 (1996).
[9] A. Keren, Phys. Rev. B **50**, 10 039 (1994).
[10] F. Mezei and A. P. Murani, J. Magn. Magn. Mater. **14**, 211 (1979).
[11] Y. J. Uemura *et al.*, Phys. Rev. B **31**, 546 (1985).
[12] W. H. Press, B. P. Flannery, A. A. Teukolsky, and W. T. Vetterling, *Numerical Recipes* (Cambridge University Press, Cambridge, 1989).
[13] A. Keren and G. Bazalitsky, Physica B **289**, 205 (2000).
[14] L. P. Lévy and A. T. Ogielski, Phys. Rev. Lett. **57**, 3288 (1986); L. P. Lévy, Phys. Rev. B **38**, 4963 (1988).
[15] T. McMullen and E. Zaremba, Phys. Rev. B **18**, 3026 (1978).